THE JOURNAL OF COMPARATIVE NEUROLOGY 461:49–60 (2003)

Localization of [^{3}H]Nicotine, [^{3}H]Cytisine, [^{3}H]Epibatidine, and [^{125}I]α-Bungarotoxin Binding Sites in the Brain of *Macaca mulatta*

ZHI-YAN HAN,[1] MICHELE ZOLI,[2] ANA CARDONA,[3] JEAN-PIERRE BOURGEOIS,[1] JEAN-PIERRE CHANGEUX,[1]* AND NICOLAS LE NOVÈRE[1]
[1]CNRS URA 2182–"Récepteurs et Cognition," Institut Pasteur, 75724 Paris Cedex 15, France
[2]Department of Biomedical Sciences, Section of Physiology, University of Modena and Reggio Emilia, 41100 Modena, Italy
[3]"Recherche et Expertise en Histotechnologie et Pathologie," Institut Pasteur, 75724 Paris Cedex 15, France

ABSTRACT

We determined the localization of [^{3}H]nicotine, [^{3}H]cytisine, [^{3}H]epibatidine, and [^{125}I]α-bungarotoxin binding sites in the brain of rhesus monkey by means of receptor autoradiography. The labelings by [^{3}H]nicotine, [^{3}H]cytisine, and [^{3}H]epibatidine were highly concordant, except for epibatidine. Layer IV of some cortical areas, most thalamic nuclei, and presubiculum displayed high levels of labeling for the three ligands. Moderate levels of binding were detected in the subiculum, the septum, and the mesencephalon. Low levels were present in layers I–II and VI of the cortex, the cornu Ammonis, the dentate gyrus, and the amygdala. In addition, the level of epibatidine labeling was very high in the epithalamic nuclei and the interpeduncular nucleus, whereas labeling by nicotine and cytisine was very weak in the same regions. The distribution of [^{125}I]α-bungarotoxin binding differed from the binding of the three agonists. The labeling was dense in layer I of most cortical areas, dentate gyrus, stratum lacunosum-moleculare of CA1 field, several thalamic nuclei, and medial habenula. A moderate labeling was found in layers V and VI of the prefrontal and frontal cortices, layer IV of primary visual cortex, amygdala, septum, hypothalamus, and some mesencenphalic nuclei. A weak signal was also detected in subiculum, claustrum, stratum oriens, and stratum lucidum of cornu Ammonis and also in some mesencephalic nuclei. The distribution of nicotine, cytisine, and epibatidine bindings corresponds broadly to the patterns observed in rodents, with the marked exception of the epithalamus. However, in monkey, those distributions match the distribution of α2 messenger RNA, rather than that of α4 transcripts as it exists in rodent brains. The distribution of the binding sites for α-bungarotoxin is larger in the brain of rhesus monkeys than in rodent brain, suggesting a more important role of α7 receptors in primates. J. Comp. Neurol. 461:49–60, 2003.

Indexing terms: nicotinic acetylcholine receptors; nicotinic ligands; cerebral cortex

The nicotinic acetylcholine receptors (nAChRs) are well-characterized transmembrane allosteric proteins involved in the fast responses to acetylcholine (Corringer et al., 2000; Karlin, 2002). They are composed of five identical (homopentamers) or different (heteropentamers) polypeptide chains arranged symmetrically around an axis perpendicular to the membrane. The agonist binding sites are located at the interface between two subunits. In mammalian neurons, the combinatorial assembly of the subunits (α2–7,β2–4) generates a wide diversity of receptors, with various electrical and binding properties (Role and Berg, 1996; Le Novère et al., 2002).

nAChRs are essential to numerous brain functions and accordingly have been implicated in several human neu-

Grant sponsor: Collège de France; Grant sponsor: Association pour la Recherche contre le Cancer; Grant sponsor: European Union.

*Correspondence to: Jean-Pierre Changeux, CNRS URA 2182–"Récepteurs et Cognition," Institut Pasteur, 75724 Paris Cedex 15, France. E-mail: changeux@pasteur.fr

Received 28 October 2002; Accepted 6 January 2003

DOI 10.1002/cne.10659

Published online the week of April 28, 2003 in Wiley InterScience (www.interscience.wiley.com).

rologic and psychiatric diseases, either during the pathogenic process or in the generation of the symptomatology (Gotti et al., 1997; Léna and Changeux, 1997). In addition of their role as the main relay in the motor autonomic transmission, neuronal nAChRs are strongly involved in many cognitive processes (Levin and Simon, 1998) as well as sensory, limbic, and autonomic functions (such as treatment of sensory input, regulation of mood, and nociception).

The involvement of nAChRs in brain functions and malfunctions is multiple and is still poorly understood. Several mutations in the genes encoding α4 or β2 subunits have been identified as a cause of neocortical epilepsy (Steinlein et al., 1995, 1997; De Fusco et al., 2000). Nicotine has a positive effect on memory processes, which are impaired in mice carrying the inactivation of the subunit β2 (Picciotto et al., 1995). Those mice present an increased neurodegeneration during aging, together with a decrease of cognitive performances (Zoli et al., 1999). nAChRs are also thought to be involved in several types of dementia, such as Parkinson's and Alzheimer's diseases (Quik et al., 2000b; Court et al., 2001). nAChRs have been repeteadly implicated in schizophrenic syndromes. An abnormally high proportion of schizophrenic patients is composed of heavy smokers and nicotine has been successfully used to relieve their symptoms. nAChRs antagonists mimic schizophrenic features in animal models. Moreover, the α7 gene was found to be significantly linked to the syndrome in one family (Freedman et al., 1997; Adler et al., 1998). Finally, neuronal nAChRs, particularly those expressed in the basal ganglia, are thought to be responsible for nicotine dependence and therefore smoking (Picciotto et al., 1998; Di Chiara, 2000).

To clarify the anatomical bases for the involvement of the various nAChR isoforms in the function of specific brain circuits, much work has been devoted to the study of the precise localization of nAChRs in the central and peripheral nervous systems. A technique of choice is receptor autoradiography, which allows mapping out, in a quantitative or semiquantitative fashion, the distribution of binding sites for nicotinic ligands.

Saturation binding experiments performed on reconstituted systems showed that there are two main populations of neuronal nAChRs. Homopentameric α7 nAChRs bind the snake α-bungarotoxin with high affinity (Couturier et al., 1990; Schoepfer et al., 1990; Chen and Patrick, 1997), whereas heteropentameric nAChRs (composed of different combinations of α2–6 and β2–4 subunits) are insensitive to this toxin (Boulter et al., 1987). On the other hand, α7 nAChRs bind the small agonists nicotine, cytisine, and epibatidine with a lower affinity than most of the heteropentameric receptors (Whiting et al., 1991; Anand et al., 1993; Wang et al., 1996). Among the neuronal heteropentameric receptors, pharmacological heterogeneity has been demonstrated (Parker et al., 1998).

Receptor autoradiography performed on the brain of transgenic mice extended the conclusions drawn from reconstituted systems to endogenous receptors. The inactivation of α7 by homologous recombination suppressed the labeling by [^{125}I]α-bungarotoxin but did not affect the labeling by [^{3}H]nicotine (Orr-Urtreger et al., 1997). Conversely, the inactivation of β2 (the most widely expressed subunit in rodent brain) suppressed the labeling by [^{3}H]nicotine in most brain regions (Picciotto et al., 1995) but did not affect the labeling by [^{125}I]α-bungarotoxin (Zoli et al., 1998). The inactivation of α4, α6, and β2 revealed heterogeneity among the distributions of binding sites for [^{3}H]nicotine, [^{3}H]cytisine, and [^{3}H]epibatidine (Zoli et al., 1998; Marubio et al., 1999; Ross et al., 2000; Champtiaux et al., 2002) and permitted us to assign binding patterns tentatively to subsets of receptors.

In addition, detailed autoradiography experiments have been performed in wild-type rodents (Clarke et al., 1984, 1985; Härfstrand et al., 1988; Pauly et al., 1989; Happe et al., 1994; Perry and Kellar, 1995), and some more partial surveys have been carried out in primates (Cimino et al., 1992; Perry et al., 1992; Rubboli et al., 1994; Breese et al., 1997; Spurden et al., 1997; Sihver et al., 1998; Court et al., 2000a). Modifications of ligand binding have also been investigated in the brain of humans with neuropsychiatric diseases (Freedman et al., 1995; Perry et al., 1995; Court et al., 1999, 2000b, 2001; Sihver et al., 1999). Here we describe an extensive autoradiographic mapping of [^{3}H]nicotine, [^{3}H]cytisine, [^{3}H]epibatidine, and [^{125}I]α-bungarotoxin binding sites in the brain of the rhesus monkey.

MATERIALS AND METHODS

Chemicals

(–)-[N-methyl-^{3}H]nicotine, [^{3}H]cytisine, [^{3}H]epibatidine, and [^{125}I]α-bungarotoxin were purchased from Amersham Biosciences (Little Chalfont, United Kingdom). Unlabeled (–)-nicotine bitartrate and other drugs were purchased from Sigma (St. Louis, MO).

Animal brains

The brains of three adult (approximately aged 15 years) male rhesus monkeys (*Macaca mulatta*) were obtained from the Institut Cognitif in Lyon, France. The animals were treated as described by Han et al. (2000). They were tranquilized with ketamine (0.1 ml · kg^{-1}) and deeply anesthetized with sodium phenobarbital (40 mg · kg^{-1}, with a solution at 50 mg · ml^{-1}), prior to transcardiac perfusion with 500 ml of ice-cold saline solution. Maintenance of animals and the procedures for euthanasia were performed according to the recommendations of the Centre National de la Recherche Scientifique ethical committee for animal care and manipulation. The brain was then dissected out from the skull and sectioned into several pieces of about 30 × 40 × 40 mm. The pieces were immediately frozen in dry ice powder and kept at −80°C until use.

Receptor autoradiography

Fourteen-micrometer-thick sections were cut on a cryostat and mounted on Superfrost slides. They were dried at room temperature for 20 minutes and then stored at −80°C for under 3 days. On the day of the experiment, the slides were brought to room temperature and processed according to established protocols (Clarke et al., 1985; Happe et al., 1994; Perry and Kellar, 1995; Zoli et al., 1998).

[^{3}H]nicotine (84 Ci · mmol^{-1}) was used at a concentration of 5 nM. The incubation was performed at room temperature for 30 minutes in 50 mM Tris-HCl, pH 7.4. It was followed by four rinses of 30 seconds each in the same buffer, followed by a brief rinse in distilled water, all performed at 4°C. Nonspecific binding was defined as

binding in the presence of an excess of cold nicotine (10 μM). The film exposure time was 3–5 months.

[^{3}H]cytisine (30 Ci · mmol^{-1}) was used at a concentration of 5 nM. The incubation was performed at 4°C for 60 minutes in 50 mM Tris-HCl, pH 7.4, containing 120 mM NaCl, 5 mM KCl, 2.5 mM $CaCl_2$, and 1 mM $MgCl_2$. This was followed by three rinses for 2.5 minutes each in 50 mM Tris-HCl, pH 7.4, followed by a brief rinse in distilled water, all performed at 4°C. Nonspecific binding was defined as binding in the presence of an excess of cold nicotine (10 μM). The film exposure time was 3–5 months.

[^{3}H]epibatidine (56 Ci · mmol^{-1}) was used at a concentration of 200 pM. The incubation was performed at room temperature for 30 minutes in 50 mM Tris-HCl, pH 7.4, followed by two rinses of 5 minutes each in the same buffer, followed by a brief rinse in distilled water, all performed at 4°C. Nonspecific binding was defined as binding in the presence of and excess of cold nicotine (10 μM). The film exposure time was 3–5 months;

[^{125}I]α-bungarotoxin (2,500 Ci · mmol^{-1}) was used at a concentration of 1.5 nM. The preincubation and incubation were performed at room temperature for 30 and 120 minutes, respectively, in 50 mM Tris-HCl, pH 7.4, containing 0.1% bovine serum albumin. This was followed by six rinses of 30 minutes each in 50 mM Tris-HCl, pH 7.4, and a brief rinse in distilled water, all performed at 4°C. Nonspecific binding was defined as binding in the presence of cold nicotine (1 mM). The film exposure time was 2–3 days.

Slides were exposed to [^{3}H]Hyperfilm (Amersham) for the length of time indicated and developed in Kodak D19 film developer (3 minutes 30 seconds at 22°C). Alternatively, slides were exposed to a β imager (BioSpace, Paris, France), which directly measures the radioactive disintegrations (Crumeyrolle-Arias et al., 1996).

Photomicrograph production

Film autoradiograms were digitized with a black-and-white Hamamatsu CCD camera. β Imager results were transformed into gray-scale images with the apparatus's dedicated software. Figures were constructed within Photoshop (Adobe Systems Inc, San Jose, CA) and the open-source software The Gimp (http://www.gimp.org).

Analysis of histological preparations

Analysis of the labeling patterns was carried out on autoradiograms. To help in the identification of anatomical structures, the sections were counterstained with toluidine blue. The rostrocaudal distribution of the labeling provided by each ligand was analyzed in coronal sections, a detailed regional analysis being carried out based on the cynomolgus monkey brain atlas (Szabo and Cowan, 1984) and the rhesus monkey brain atlas by Paxinos et al. (2000). For each ligand, the intensity of the labeling, if not null, was ranked from (+), barely detectable, to ++++, very strong, corresponding to the most well-labeled structure. Hence, the relative values of different ligands cannot be directly compared with each other.

RESULTS

The autoradiography experiments carried out on the brains of three different rhesus monkeys provided similar results. No ligand gave a detectable labeling when an excess of cold nicotine was added to the incubation mixture.

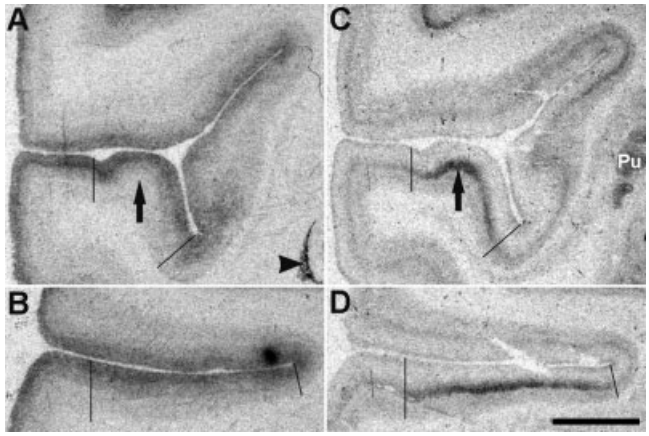

Fig. 1. Film autoradiograms of [^{125}I]α-bungarotoxin (**A,B**) and [^{3}H]epibatidine (**C,D**) binding in the auditory cortex at levels Bregma –9 mm (A,C) and Bregma –17 mm (B,D). Primary auditory cortex is delimited by lines. Arrows point to layer IV of the auditory primary cortex. Arrowhead points to the reticular thalamic nucleus. Pu, putamen. Scale bar = 5 mm.

Telencephalon

Although the intensity of [^{3}H]nicotine labeling was much lower than the intensity of [^{3}H]cytisine and [^{3}H]epibatidine labeling, the overall patterns of labeling by the ligands in the neocortex were similar. In contrast, the labeling by [^{125}I]α-bungarotoxin had a very different distribution. The signals were found throughout the entire neocortex, their intensities and laminar distributions displaying regional variations.

The binding of small agonists in layer I was barely detectable, regardless of the cortical region. In contrast, the [^{125}I]α-bungarotoxin labeling was strong in layer I all over the cortex except in the secondary auditory area (insular cortex and prokoniocortex), where it was moderate (Fig. 1). The binding of [^{125}I]α-bungarotoxin was barely detectable in granular layer IV, except in the primary visual cortex, where the signal was moderate (Fig. 2). The binding of [^{3}H]nicotine in layer IV was moderate in the primary sensory cortices and weak, although clear, in every other area. The binding of [^{3}H]cytisine and [^{3}H]epibatidine was moderate in layer IV everywhere, except in the primary cortices, where it was stronger. In particular, the visual and auditory koniocortices, where layer IV is thicker, were sharply distinct from the surrounding secondary sensory areas. In the primary auditory cortices (Fig. 1), the boundaries of the labeling corresponded to those of the domain of high acetylcholinesterase activity (Morel et al., 1993). The supragranular layers displayed a moderate signal for the binding of [^{125}I]α-bungarotoxin, except in the cingulate, frontal, and prefrontal cortices and the secondary auditory area, where the signal was weak. The binding of small agonists was barely detectable in the supragranular layers except for the frontal regions, where a weak signal was detected in layer III. The infragranular layers displayed a weak labeling for the binding of [^{125}I]α-bungarotoxin, except in the frontal and prefrontal regions, where the signal was moderate. The binding of

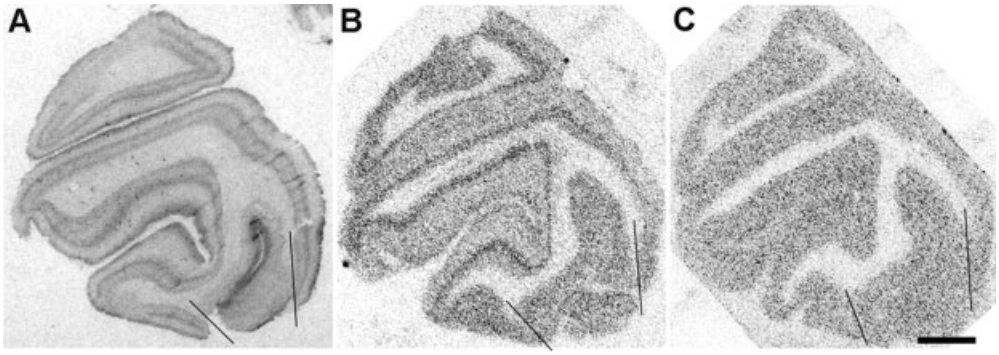

Fig. 2. Autoradiograms of [^{125}I]α-bungarotoxin (**A**), [^{3}H]epibatidine (**B**), and [^{3}H]nicotine (**C**) binding in the area V1 and V2 of the visual cortex at level Bregma –47 mm. V1 and V2 visual cortex areas are delimited by lines. Note the binding of bungarotoxin in layer IV of area V1 but not in area V2. The binding of [^{125}I]α-bungarotoxin was revealed on a film, whereas the binding of [^{3}H]epibatidine and [^{3}H]nicotine was revealed with the β imager. Scale bar = 5 mm.

small agonists was weak but clear in the layer VI and barely detectable in the layer V all over the cortex.

The binding of small agonists, therefore, provided roughly three kinds of laminar distribution, according to the intensity in layer IV. The first pattern was obviously present in the agranular areas (no layer IV). The second pattern was present in the primary sensory cortices, displaying a strong labeling in layer IV. The remaining areas analyzed displayed a moderate labeling in layer IV. The laminar distribution of [^{125}I]α-bungarotoxin binding was extremely variable and made up at least seven patterns (details in Table 1).

Area 29 of the retrosplenial cortex presents a specific laminar architecture, with a large granular layer III–IV and almost absent supragranular layers (Morris et al., 1999). [^{125}I]α-bungarotoxin gave a strong labeling in layer I and a weak labeling in the infragranular layers. The small agonists gave very strong labeling in the granular layer (nicotine labeling was less intense than cytisine and epibatidine labeling) and a weak labeling in the infragranular layers (Fig. 3).

Hippocampus was devoid of [^{3}H]nicotine labeling. The binding of [^{3}H]cytisine and [^{3}H]epibatidine was weak and restricted to the stratum lacunosum of CA fields (Fig. 4). On the contrary, we found a clear and diverse labeling by [^{125}I]α-bungarotoxin throughout the hippocampal formation. The granular layer of the dentate gyrus displayed a strong signal, whereas the labeling in the polymorph layer was weak. [^{125}I]α-bungarotoxin binding was moderate in the pyramidal layer of CA1 and CA2 and in the stratum lacunosum-moleculare of CA2 and CA3. It was stronger in the stratum lacunosum-moleculare of CA1. The subiculum displayed a moderate labeling of the small ligands and a weak, but clear, labeling of [^{125}I]α-bungarotoxin. The labeling in the presubiculum revealed a laminar pattern consistent with the immunocytochemistry of choline acetyltransferase (see Fig. 1G of Alonso and Amaral, 1995). The medial and external layers were strongly labeled by [^{3}H]cytisine and [^{3}H]epibatidine. [^{3}H]nicotine labeling was stronger in the medial than in the external layer, whereas the binding of [^{125}I]α-bungarotoxin was stronger in the external than in the medial layer.

All nuclei of the amygdala showed a very weak level of binding for the small agonists, whereas binding for [^{125}I]α-bungarotoxin was moderate, except in the medial nucleus (high labeling) and the basolateral nucleus (weak labeling). The labeling was heterogeneous in the septum and basal forebrain nuclei for all the ligands. The binding of the agonists was barely detectable, except in the lateral dorsal nucleus, the posterior part of the lateral ventral nucleus, the medial septum, and the bed nucleus of the stria terminalis. Only a small posterolateral part of the latter was in fact labeled. The binding of [^{125}I]α-bungarotoxin was found mainly in the posterior part of the lateral intermediate nucleus and in the cholinergic nuclei, i.e., the basal nucleus of Meynert, the diagonal band, and the medial septum, the latter being the only nucleus of the basal forebrain/septal region to display labeling for all the four ligands.

The forebrain basal ganglia were found to be devoid of [^{125}I]α-bungarotoxin labeling, except for the claustrum and the medullary lamina, the fiber shell connecting the internal to the external globus pallidus. On the contrary, the agonists displayed a clear labeling in the entire striatum (Figs. 1, 4, 5). However, a major difference in the intensity of labeling for the three agonists was observed in striatum, [^{3}H]epibatidine labeling being stronger than [^{3}H]cytisine and [^{3}H]nicotine labeling (see, e.g., in Fig. 5, the striatal labeling for [^{3}H]epibatidine, higher than labeling in layers V–VI of the frontal cortex, whereas both regions have identical labeling intensity for [^{3}H]nicotine).

Diencephalon

Binding of [^{125}I]α-bungarotoxin was found throughout the hypothalamus, except in the lateral area. On the contrary, a weak binding for the agonists was found only in the lateral and posterior area, with a strong binding in the mammillary nuclei, where the [^{125}I]α-bungarotoxin binding was weak.

The anterior group of thalamic nuclei displayed a very strong binding for the agonists, except for the anterodorsal nuclei, which displayed a moderate signal. Although the binding of [^{125}I]α-bungarotoxin was very strong in the anteroventral and anteromedial nuclei, it was weak in the parathenial nucleus, contrary to the binding of agonists. The ventral and mediodorsal groups of thalamic nuclei displayed signals ranging from moderate to strong for the agonists. However, only weak [^{125}I]α-bungarotoxin labeling was detected in the ventral group and a moderate labeling in the mediodorsal group. The intralaminar nu-

clei, separating the mediodorsal from the ventral group, were devoid of signal for any of the ligands. The reticular thalamic nucleus was labeled moderately by the agonists but strongly by the [^{125}I]α-bungarotoxin (Figs. 4, 6). The parafascicular and the centromedian nuclei displayed a very weak labeling for the agonists but a strong labeling for the [^{125}I]α-bungarotoxin in the centromedian nucleus (Fig. 6). Finally, the geniculate nuclei displayed a moderate to strong binding for all the four ligands (Fig. 4).

The epithalamus provided contrasting results, possibly because of the extreme diversity of nAChRs subunits expressed in this region (Han et al., 2000). The pineal gland was labeled only by [^{3}H]epibatidine. The signal observed in the lateral habenula was at best very weak, whatever the ligand considered (Fig. 7). In the medial habenula, [^{3}H]epibatidine gave a strong signal throughout the entire structure. The same distribution was observed with the [^{125}I]α-bungarotoxin except for the anteromedial part, where the signal was moderate. [^{3}H]cytisine gave a moderate labeling restricted to the anterolateral part. Finally, [^{3}H]nicotine barely labeled the medial habenula. The fasciculus retroflexus, carrying axonal projections from the habenula to the interpeduncular nucleus, was heavily labeled by [^{3}H]epibatidine and only by this ligand (Fig. 6).

Mesencephalon

Only the anterior part of the mesencephalon was included in the present study, up to the level of Bregma –18 mm. The interpeduncular nucleus was very strongly labeled by [^{3}H]epibatidine. The labeling for [^{3}H]cytisine was moderate, and the labeling for [^{3}H]nicotine was weak. No labeling for [^{125}I]α-bungarotoxin could be observed in the interpeduncular nucleus.

The substantia nigra pars compacta was moderately labeled by [^{3}H]epibatidine and [^{3}H]cytisine and weakly by [^{3}H]nicotine. The pattern of labeling in the ventral tegmental area was similar but weaker than that in the substantia nigra.

The tectum revealed a labeling for all the ligands, particularly in the superior granular region. The small ligands moderately labeled other nuclei, such as the shell of the red nucleus, whereas a clear and sometimes strong signal was detected in the oculomotor nuclei.

DISCUSSION

We report here a systematic mapping of the high affinity binding sites for three nicotinic agonists, [^{3}H]nicotine, [^{3}H]cytisine, and [^{3}H]epibatidine, and for one nicotinic blocker, [^{125}I]α-bungarotoxin, in the brain of the rhesus monkey.

Methodological aspects

Receptor autoradiography is performed after binding at equilibrium. Hence, it reveals mainly high-affinity desensitized receptors. Under those conditions, adequate concentrations of ligands permit discrimination between receptor subtypes that exhibit desensitized states with very different affinities, even if higher concentrations of the same ligand could also reveal low-affinity populations. For the experiments presented here, we selected the ligand concentrations used in the autoradiographic survey of nicotinic ligands in the mouse brain (Zoli et al., 1998). They are close to the concentrations classically used in studies conducted either on rodents or on humans. Indeed, the available data do not exhibit major differences in the pharmacology for classical nicotinic ligands between rodent (Parker et al., 1998) and primate (Gopalakrishnan et al., 1996; Stauderman et al., 1998) recombinant receptors. However, a precise assessment of the equilibrium binding parameters of native nAChR subtypes in the monkey is not available. In addition, the characteristics of allosteric transitions, which affect the apparent affinity of receptors, are also unknown. Therefore, the ligand concentrations used in this study may not be optimal for the autoradiographic visualization of all nAChR subtypes in primates (see below for discussion of nicotinic agonist binding of α4β2 receptors).

Overall conservation of the pattern of [^{3}H]nicotine, [^{3}H]cytisine, and [^{3}H]epibatidine binding between rodents and primates

Comparison of the results in the present study and the results of previous receptor autoradiography surveys performed in rodents (Clarke et al., 1985; Härfstrand et al., 1988; Fuchs, 1989; Pauly et al., 1989; Happe et al., 1994; Perry and Kellar, 1995; Zoli et al., 1998) and primates (Cimino et al., 1992; Perry et al., 1992; Rubboli et al., 1994; Breese et al., 1997; Spurden et al., 1997; Sihver et al., 1998; Court et al., 2000a) shows that the distribution of the binding sites for the small nicotinic agonists is well conserved between rodent and monkey brains. Moreover, there is good agreement among the distributions of the binding sites for the three agonists, with the exception of the habenulointerpeduncular system (see below).

A few previous studies have dealt with the distribution of [^{3}H]nicotine or [^{3}H]cytisine binding site in primate brain. In general, our results agree with these studies. The highest levels of binding were detected in the thalamus of both monkey and human brains (Cimino et al., 1992; Rubboli et al., 1994; Perry and Kellar, 1995; Spurden et al., 1997), whereas moderate levels were observed in the striatum and the neocortex of human (Spurden et al., 1997) but not of monkey (Cimino et al., 1992). We report here a weak signal in striatum. The lack of detection of [^{3}H]nicotine binding previously observed in monkey striatum could be due to a lower sensitivity of the technique used by the previous authors. However, our results are consistent with the binding of epibatidine and cytisine and also agree well with the results in human.

In the neocortex, as shown in former work (Perry et al., 1992; Spurden et al., 1997), the labeling was concentrated in layer IV, which is the target of acetylcholinesterase-positive thalamocortical afferents (Kageyama et al., 1990; Morel et al., 1993; Alonso and Amaral, 1995; Alonso et al., 1996; Broides et al., 1996). With regard to the hippocampal formation, very high levels of [^{3}H]cytisine and [^{3}H]epibatidine binding were detected in the presubiculum and moderate in subiculum, again in agreement with previous studies in the human brain (Perry et al., 1992; Rubboli et al., 1994).

Distribution of α-bungarotoxin binding is wider in monkey than in rodents

Here, we present an extensive mapping of [^{125}I]α-bungarotoxin binding sites throughout the mid- and forebrain using an homogeneous protocol that allows mean-

TABLE 1. Regional [^{3}H]Nicotine (Nic), [^{3}H]Cytisine (Cyt), [^{3}H]Epibatidine (Epi), and [^{125}I]α-Bungarotoxin (BTX) Binding in the Brain of Monkey[1]

	[^{3}H]Nic	[^{3}H]Cyt	[^{3}H]Epi	[^{125}I]α-BTX
Telencephalon				
Retrosplenial cortex area 29				
Layer I	(+)	(+)	(+)	+++
Layers III–IV	+++	++++	++++	(+)
Layers V–VI	+	+	+	+
Area 24 of anterior cingulate cortex				
Layer I	(+)	(+)	(+)	+++
Layers II–III	(+)	(+)	(+)	+
Layers V–VI	(+)	+	+	++
Area 23 of anterior cingulate cortex				
Layer I	(+)	(+)	(+)	+++
Layers II–III	(+)	(+)	(+)	+
Layer IV	+	++	++	(+)
Layers V–VI	(+)	+	+	++
Prefrontal cortex				
Layer I	(+)	(+)	(+)	+++
Layers II–III	(+)	(+)	(+)	+
Layer IV	+	++	++	+
Layer V	(+)	(+)	(+)	++
Layer VI	(+)	+	+	++
Frontal cortex				
Layer I	(+)	(+)	(+)	+++
Layer II	(+)	(+)	(+)	+
Layer III	(+)	+	+	+
Layer V	(+)	(+)	(+)	++
Layer VI	(+)	+	+	++
Somato-sensory cortex				
Layer I	(+)	(+)	(+)	+++
Layers II–III	(+)	(+)	(+)	++
Layer IV	+	+++	+++	(+)
Layer V	(+)	(+)	(+)	+
Layer VI	(+)	+	+	+
Parietal cortex				
Layer I	(+)	(+)	(+)	+++
Layers II–III	(+)	(+)	(+)	++
Layer IV	+	++	++	(+)
Layer V	(+)	(+)	(+)	+
Layer VI	(+)	+	+	+
Insular cortex				
Layer I	(+)	(+)	(+)	++
Layers II–III	(+)	(+)	(+)	+
Layer IV	+	++	++	(+)
Layer V	(+)	(+)	(+)	+
Layer VI	(+)	+	+	+
Prokoniocortex				
Layer I	(+)	(+)	(+)	++
Layers II–III	(+)	(+)	(+)	+
Layer IV	+	++	++	(+)
Layer V	(+)	(+)	(+)	+
Layer VI	(+)	+	+	+
Auditory koniocortex				
Layer I	(+)	(+)	(+)	+++
Layers II–III	(+)	(+)	(+)	++
Layer IV	++	+++	+++	(+)
Layer V	(+)	(+)	(+)	+
Layer VI	(+)	+	+	+
Temporal cortex (except auditory cortices)				
Layer I	(+)	(+)	(+)	+++
Layers II–III	(+)	(+)	(+)	++
Layer IV	+	++	++	(+)
Layer V	(+)	(+)	(+)	+
Layer VI	(+)	+	+	+
Visual cortex VI				
Layer I	(+)	(+)	(+)	+++
Layers II–III	(+)	(+)	(+)	(+)
Layer IV	+	+++	+++	++
Layer V	(+)	(+)	(+)	+
Layer VI	(+)	+	+	++
Visual cortex V2				
Layer I	(+)	(+)	(+)	+++
Layers II–III	(+)	(+)	(+)	+
Layer IV	+	++	++	(+)
Layer V	(+)	(+)	(+)	+
Layer VI	(+)	(+)	(+)	+
Hippocampal formation				
Dentate gyrus				
Granular layer	−	−	−	+++
Polymorph layer	−	−	−	+
CA1 field				
Stratum oriens	−	−	−	+
Pyramidal cell layer	−	−	−	++
Strata lucidum and radiatum	−	−	−	+
Stratum lacunosum-moleculare	−	+	+	+++
CA2 field				
Stratum oriens	−	−	−	+
Pyramidal cell layer	−	−	−	++
Strata lucidum and radiatum	−	−	−	+
Stratum lacunosum-moleculare	−	+	+	++
CA3 field				
Stratum oriens	−	−	−	+
Pyramidal cell layer	−	−	−	+
Strata lucidum and radiatum	−	−	−	+
Stratum lacunosum-moleculare	−	+	+	++
CA4	−	−	−	+
Subiculum	++	++	++	+
Presubiculum				
External layer	+	+++	+++	++
Medial layer	++	+++	+++	(+)
Internal layer	−	−	−	(−)
Amygdala				
Central nucleus	(+)	(+)	(+)	++
Medial nucleus	(+)	(+)	(+)	+++
Lateral nucleus	(+)	(+)	(+)	++
Hippocampal area	(+)	(+)	(+)	++
Basolateral nucleus	(+)	(+)	(+)	+
Septum and basal forebrain				
Lateral dorsal septum	++	++	++	−
Lateral intermediate septum, anterior	(+)	(+)	(+)	−
Lateral intermediate septum, posterior	(+)	(+)	(+)	++
Lateral ventral septum, anterior	(+)	(+)	(+)	−
Lateral ventral septum, posterior	+	++	++	−
Medial septum	+	++	++	+++
Diagonal band	+	+	+	++
Substantia innominata	(+)	(+)	+	+
Septofimbrial nucleus	(+)	(+)	(+)	++
Septofimbrial organ	(+)	(+)	(+)	++
Bed nucleus of the stria terminalis	+	+++	+++	++
Basal nucleus of Meynert	(+)	(+)	(+)	++
Forebrain basal ganglia				
Putamen	+	+	++	−
Caudate nucleus	+	+	++	−
Accumbens nucleus	+	+	++	−
Ventral pallidum	+	+	++	−
Globus pallidus	−	−	−	−
medullary lamina	−	−	−	++
Claustrum	+	+	+	+
Diencephalon				
Optic tract	−	(+)	++	−
Hypothalamus				
Median preoptic nucleus	−	−	−	+
Lateral preoptic area	−	−	−	++
Paraventricular nucleus, parvicellular	−	−	−	+++
Supraoptic nucleus	−	−	−	++
Ventro-medial nucleus	−	−	−	++
Anterior area	−	−	−	++
Posterior area	+	+	+	++
Lateral area	+	+	+	−
Mammillary nucleus	++	+++	+++	+
Thalamus				
Anteroventral nucleus	++++	++++	++++	+++
Anterodorsal nucleus	++	++	++	++
Anteromedial nucleus	++++	++++	++++	+++
Parathenial nucleus	+++	+++	+++	+
Paraventricular nucleus	+	+	+	−
Interanteromedial nucleus	++++	++++	++++	++
Intermediodorsal nucleus	+	+	+	+
Intralaminar nuclei	−	−	−	−
Reuniens nucleus	++	++	++	+
Reticular nucleus	++	++	++	+++
Zona incerta	+	+	+	+
Ventral anterior nucleus	+++	+++	+++	+
Ventral lateral nucleus	+++	+++	+++	+
Ventral posterolateral nucleus	++	++	++	+
Ventral posteromedial nucleus	+++	+++	+++	+
Medial dorsal nucleus, lateral	++	++	++	++
Medial dorsal nucleus, central	+++	+++	+++	++
Medial dorsal nucleus, medial	++	++	++	++
Medial dorsal nucleus, dorsal	+++	+++	+++	++

TABLE 1 (continued)

	[^{3}H]Nic	[^{3}H]Cyt	[^{3}H]Epi	[^{125}I]α-BTX
Lateral dorsal superficial nucleus	+	+	+	++
Gustatory nucleus	+++	+++	+++	+++
Parafascicular nucleus	+	+	+	(+)
Centromedian nucleus	+	+	+	++++
Pulvinar	++	++	++	+++
Medial geniculate nucleus	+++	+++	+++	++
Lateral geniculate nucleus				
Layers 1 and 2	+++	+++	+++	+++
Layers 3–6	+++	+++	+++	++
Epithalamus				
Pineal gland	–	–	+++	–
Medial habenula, anterodorsolateral	(+)	+	++++	+++
Medial habenula anteroventrolateral	(+)	++	++++	++++
Medial habenula, anteromedial	(+)	+	+++	++
Medial habenula, posteromedial	(+)	+	+++	++++
Medial habenula, posterocentral	(+)	(+)	(+)	(+)
Medial habenula, posteroventrolateral	(+)	+	++++	++++
Lateral habenula medial	(+)	+	+	(+)
Lateral habenula lateral	(+)	(+)	(+)	
fasciculus retroflexus	–	–	++++	–
Mesencephalon				
Interpeduncular nucleus	+	++	++++	–
Substantia nigra, pars compacta	+	++	++	(+)
Substantia nigra, pars reticulata	–	–	–	–
Ventral tegmental area	(+)	+	+	–
Red nucleus, shell	+	++	++	+
Red nucleus, core	–	–	–	–
Medial accessory oculomotor nucleus	(+)	(+)	(+)	+
Parvicellular oculomotor nucleus	(+)	(+)	(+)	+++
Oculomotor nucleus	(+)	(+)	(+)	++
Rostral linear nucleus of the raphe	–	–	–	++
Periaqueductal gray	+	+	+	(+)
Superior colliculus				
Superficial gray layer	++	++	+++	++
Intermediate gray layer	+	+	+	+
Deep gray layer	+	+	+	+

[1]–, Not detected; (+), very weak; +, weak; ++, moderate; +++, strong; ++++, very strong.

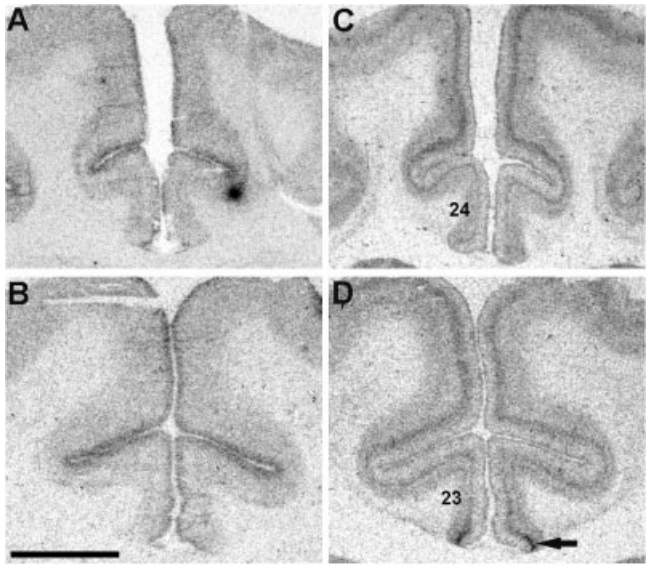

Fig. 3. Film autoradiograms of [^{125}I]α-bungarotoxin (**A,B**) and [^{3}H]epibatidine (**C,D**) binding in the cingulate and frontal cortices at levels Bregma +2 mm (A,C) and Bregma –9 mm (B,D). Note layer IV of the cingulate cortex, almost absent in the area 24 (C), but clearly visible in the area 23 (D). Arrow points to the retrosplenial areas. Scale bar = 5 mm.

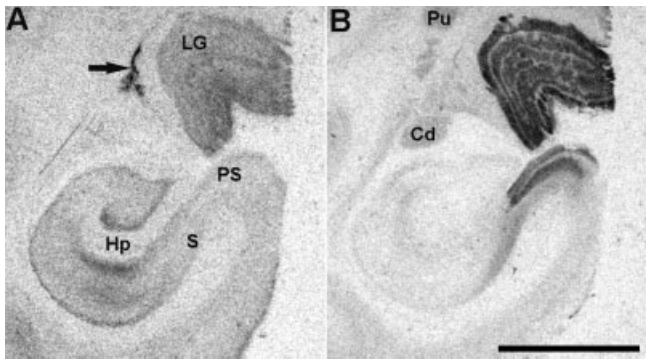

Fig. 4. Film autoradiograms of [^{125}I]α-bungarotoxin (**A**) and [^{3}H]epibatidine (**B**) binding in the hippocampus and lateral geniculate at level Bregma –15 mm. Arrow points to the the reticular thalamic nucleus. Cd, caudate nucleus; Hp, hippocampus; LG, lateral geniculate; PS, presubiculum; Pu, putamen; S, subiculum. Scale bar = 5 mm.

ingful comparisons between different areas. Previous autoradiographical studies of [^{125}I]α-bungarotoxin binding sites in primate brain were not extensive and, therefore, are sometimes difficult to compare and a fortiori with the present results. Cimino et al. (1992) found that [^{125}I]α-bungarotoxin binding was present in most thalamic areas but not in hippocampus of the monkey; Rubboli et al. (1994) found binding at high levels in human hippocampus and at low levels in human subiculum. Other autoradiographic surveys performed in humans showed that [^{125}I]α-bungarotoxin binding sites were clearly detected in supragranular layers of cortex, hippocampus, hypothalamus, red nucleus, and thalamus but at very low level except in reticular and lateral geniculate nuclei (Breese et al., 1997; Spurden et al., 1997). In the present paper, [^{125}I]α-bungarotoxin binding was found to be high in neocortex (particularly in layer I), hippocampus, and most thalamic and hypothalamic nuclei and medial habenula, and moderate in amygdala, septum, and some mesencephalic nuclei. Although these findings mostly agree with previous monkey and human studies, a striking difference between our data and human data in the thalamus is evident.

A clear difference in labeling of thalamic nuclei is also present between monkey and rodent brain, where [^{125}I]α-bungarotoxin binding was high in hippocampus, hypothalamus, some layers of neocortex, amygdala, lateral geniculate nucleus, medial habenula, and interpeduncular nucleus but almost absent from thalamus (Clarke et al., 1985; Pauly et al., 1989; Zoli et al., 1998; Whiteaker et al., 1999) or present only at weak levels (Härfstrand et al., 1988). Overall, these findings suggest that [^{125}I]α-bungarotoxin binding distribution (and α7 mRNA expression; see Han et al., 2000) in the thalamus is highly species specific in mammals, although a trend for an increase in the density of this type of nAChR can be noted for primate brain.

Previous studies have shown that, in mammalian brain, α-bungarotoxin binds only to homomeric nAChRs containing α7 subunit (Séguéla et al., 1993; Chen and Patrick, 1997; Orr-Urtreger et al., 1997). The present data on the

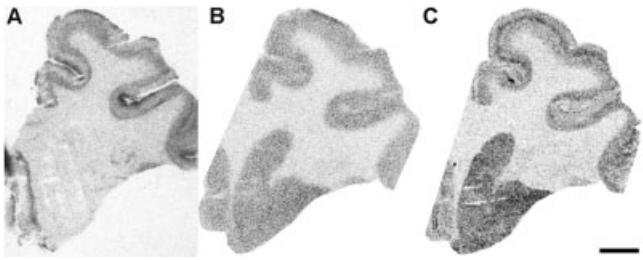

Fig. 5. Autoradiograms of [^{125}I]α-bungarotoxin (**A**), [^{3}H]nicotine (**B**), and [^{3}H]epibatidine (**C**) binding in the striatum at level Bregma +7 mm. The binding of [^{125}I]α-bungarotoxin was revealed on a film, whereas the binding of [^{3}H]epibatidine and [^{3}H]nicotine was revealed with the β imager. Note that epibatidine labeling intensity in the striatum corresponds to that present in layer IV, whereas nicotine labeling intensity in the striatum corresponds to that of infra and supragranular layers. Scale bar = 5 mm.

distribution of [^{125}I]α-bungarotoxin binding sites in the brain confirm this notion, as they match well the broad distribution of α7 subunit mRNA (Han et al., 2000). This correspondence means that, overall, most of the α-bungarotoxin binding sites are located in the somatodendritic compartment. This does not preclude the existence of some terminal populations of α7 receptors, as was demonstrated in rodents for the terminals of prefrontal pyramidal neurons located in the ventral tegmental area (Schilstrom et al., 2000). Similarly, the sharp contrast between the labeling of layers I and the labeling of II–III could mean that α-bungarotoxin binding sites are located mainly on corticocortical terminals. The more extensive distribution of [^{125}I]α-bungarotoxin binding sites parallels the wider distribution of α7 mRNA in the monkey brain in comparison with the rodent brain (Séguéla et al., 1993; Han et al., 2000). This could indicate an increased functional role of homomeric α7 receptors in primates.

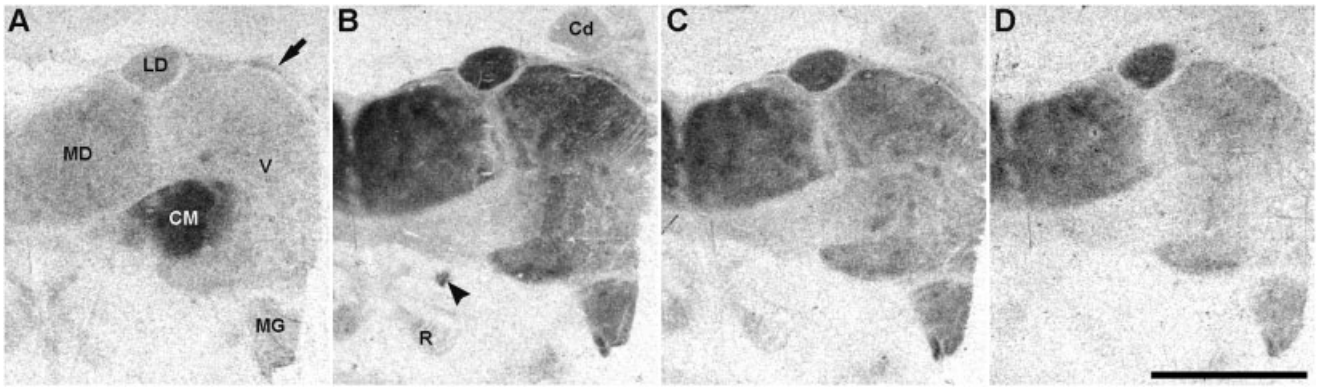

Fig. 6. Film autoradiograms of [^{125}I]α-bungarotoxin (**A**), [^{3}H]epibatidine (**B**), [^{3}H]cytisine (**C**), and [^{3}H]nicotine (**D**) binding in the thalamus at level Bregma –14 mm. Arrow points to the reticular thalamic nucleus. Arrowhead points to the fasciculus retroflexus. Cd, caudate nucleus; CM, centromedian nucleus; LD, thalamic laterodorsal nucleus; MD, thalamic mediodorsal complex; MG, medial geniculate; R, red nucleus; V, thalamic ventral complex. Scale bar = 5 mm.

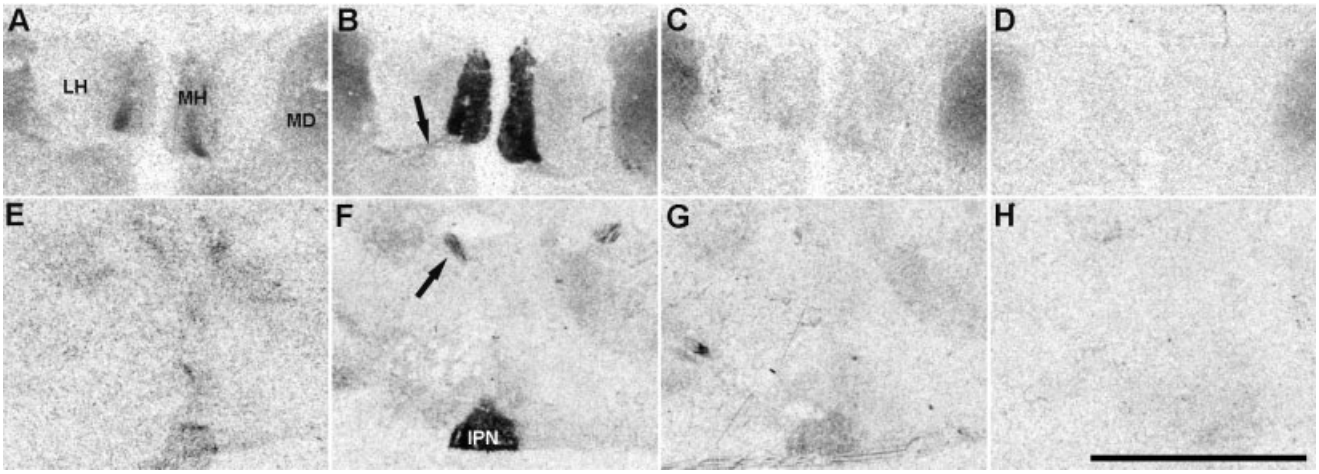

Fig. 7. Film autoradiograms of [^{125}I]α-bungarotoxin (**A,E**), [^{3}H]epibatidine (**B,F**), [^{3}H]cytisine (**C,G**), and [^{3}H]nicotine (**D,H**) binding in the habenular nuclei at level Bregma –16 mm and interpeduncular nucleus at level –13;50 mm. Arrows point to the fasciculus retroflexus. IPN, interpeduncular nucleus; LH, lateral habenula; MH, medial habenula; MD, thalamic mediodorsal complex. Scale bar = 5 mm.

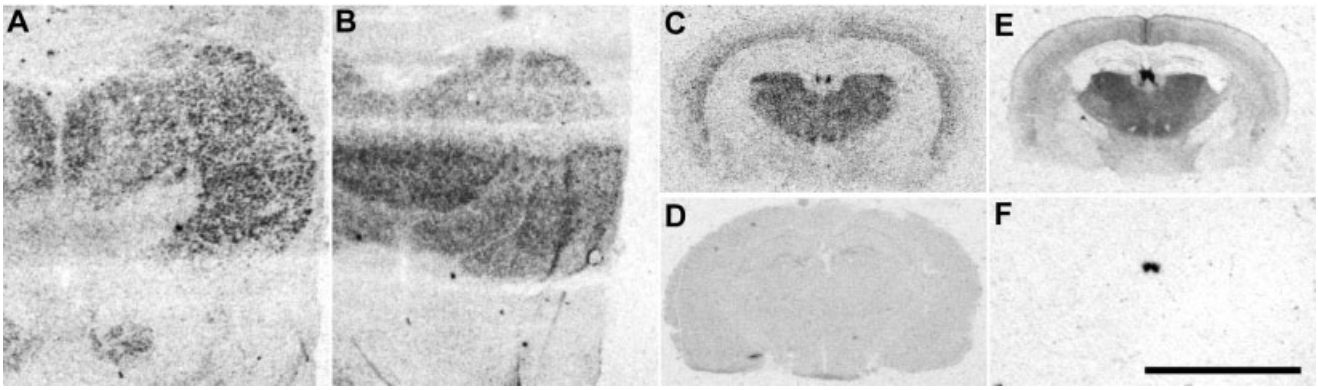

Fig. 8. Film autoradiograms showing the distribution of α2 (**A**) and α4 (**B**) subunit mRNA in the thalamus at level Bregma –14 mm (modified from Han et al., 2000). Film autoradiograms showing the distribution of α4 (**C**) and α2 (**D**) subunits mRNA in the mouse thalamus at level Bregma +1.7 m. Film autoradiograms of [^{3}H]epibatidine binding in the thalamus of wild-type (**E**) and a4$^{-/-}$ (**F**) mice at level Bregma +1.5 mm (modified from Marubio et al., 1999). Scale bar = 5 mm.

Correlation between the distribution of nicotinic agonist binding and α2 subunit

In rodents, high affinity for nicotine at saturation is attributed to receptors containing α4 and β2 subunits, based on studies performed with mutant mice (Fig. 8). Indeed nicotine concentrations similar to the one we used in the present study did not reveal any autoradiographic signal in α4$^{-/-}$ or β2$^{-/-}$ mice (Picciotto et al., 1995; Zoli et al., 1998; Marubio et al., 1999; Ross et al., 2000). In sharp contrast, in our study, we found a very weak signal for the small nicotinic agonists in the regions where α4 but not α2 mRNA has been detected (Han et al., 2000). The most striking example is the thalamic centromedian nucleus shown in Figure 6, to be compared with Figure 8A,B. On the contrary, binding for agonists is visible in the red nucleus, whereas α2 but not α4 mRNA is present. One possible explanation for this finding could be that α4* (where the star means one or several other subunits) nAChRs is mostly transported to nerve terminals, whereas α2* nAChRs remain in the somatodendritic area. Therefore, only the labeling of these latter receptors would correlate with the expression of the mRNA. However, this is unlikely. At least in rodents, there is a major colocalization of α4 mRNA and α4 immunolabeling, in particular in the thalamus (Rogers et al., 1998). Another possibility is purely methodological. The dissociation constant at equilibrium for small nicotinic ligands of monkey α4β2 receptors is unknown and could be lower than that of rodent α4β2 receptors. The concentration of nicotinic agonists used here may therefore be insufficient to visualize this receptor subtype, and, as a consequence, most [^{3}H]epibatidine, [^{3}H]cytisine, and [^{3}H]nicotine binding would correspond to α2β2 rather than to α4β2 nAChRs. Finally, desensitization properties (allosteric transition constants) could be such that not all α4β2 nAChRs are in a desensitized state under our experimental condition, decreasing the apparent affinity for the ligands.

Differences between rodent and primate habenulointerpeduncular system

Although the binding sites for these three agonists have very similar distributions in monkey brain, some exceptions are found, most notably for [^{3}H]epibatidine, whose labeling pattern is larger. The main difference was related to the nuclei belonging to the cholinergic habenulointerpeduncular system. [^{3}H]epibatidine binding was present at a high level in the medial habenula and the interpeduncular nucleus as well as in the fasciculus retroflexus, which connects the two structures. Conversely, only faint labeling for [^{3}H]nicotine and [^{3}H]cytisine was observed in the medial habenula and the fasciculus retroflexus, whereas the interpeduncular nucleus displayed no detectable signal for nicotine (Fig. 7).

In rodents, however, binding for [^{3}H]nicotine, [^{3}H]cytisine, and [^{3}H]epibatidine ranges from moderate to high, both in the medial habenula and in the interpeduncular nucleus (Clarke et al., 1985; Härfstrand et al., 1988; Happe et al., 1994; Zoli et al., 1998). The differences observed between monkey and wild-type rodents could come from the lower affinity of receptors containing α4 subunit in the monkey (see above). Although α4 subunit is (weakly) expressed in the medial habenula (Fig. 9), α4-containing receptors would not efficiently bind the agonists. On the other hand, studies in α4$^{-/-}$ and β2$^{-/-}$ knockout mice (Fig. 8) showed that [^{3}H]epibatidine strongly labels α3/6β2/4* nAChRs in the habenula, the fasciculus retroflexus, and the interpeduncular nucleus (Zoli et al., 1998; Marubio et al., 1999). The remaining signal for cytisine in the medial habenula and interpeduncular nucleus of monkey could be due to α2β2* receptors but also to α3/6β2*, exhibiting a lower affinity but present in a large amount. [^{125}I]α-bungarotoxin labels the lateral part of the medial habenula, a localization that tallies well with the pattern of expression of α7 subunit (Han et al., 2000).

The neocortex displays a large heterogeneity of binding patterns

The neocortex exhibited a large diversity of labeling patterns both for the small ligands and for the bungarotoxin. A previous article reported a survey of the laminar distribution of nicotine, cytisine, and epibatidine binding in the human brain (Sihver et al., 1998). Despite the low resolution of the images, the authors found, in agreement

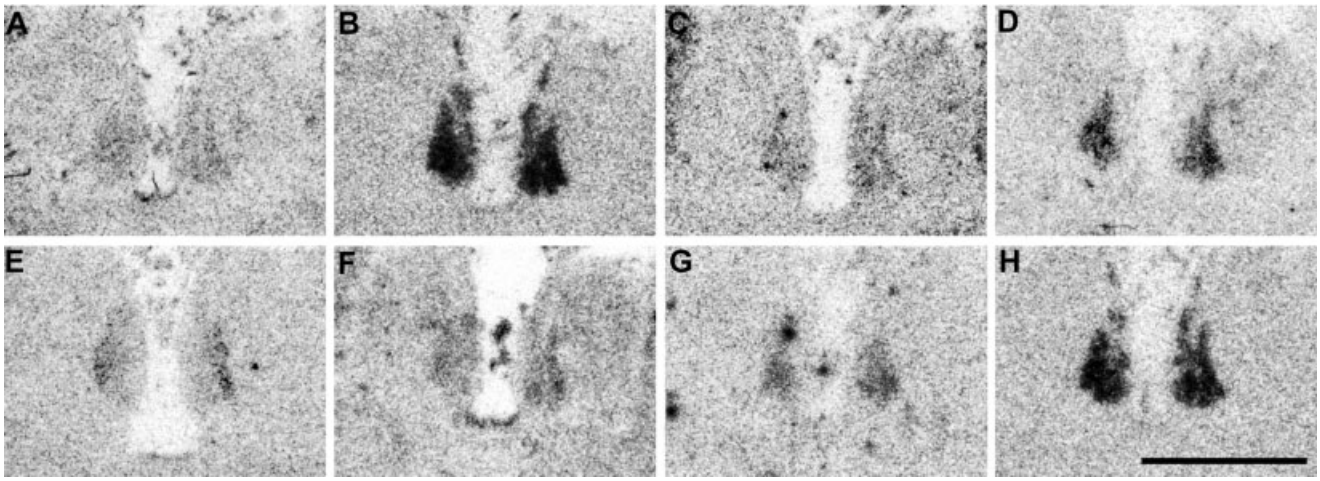

Fig. 9. Film autoradiograms showing the distribution of α2 (**A**), α3 (**B**), α4 (**C**), α6 (**D**), α7 (**E**), β2 (**F**), β3 (**G**), and β4 (**H**) subunits mRNA in adjacent coronal sections of the habenular nuclei at level Bregma –16 mm. Modified from (Han et al., 2000). Scale bar = 2.5 mm.

with the present study, widely variable laminar patterns across cortical areas. However, the interpretation of the two data sets diverges, with the main discrepancy regarding the peak of labeling, generally attributed to layer III and sometimes to layer V by those authors. There could be a difference of nAChR distribution between the cortices of humans and Old World monkeys. However, a completely different laminar pattern is unlikely. Their layer determination was based on the percentage of cortical depth. This criterion is misleading, because, in a laminar pleated structure, such as a gyrencephalic cortex, the angle of section affects the relative width of layers. For the primary auditory cortex, we unambiguously assigned the strong agonist binding to layer IV [cf. Fig. 1 and Figs. 7, 8 of Morel et al. (1993)]. Within the cingulate cortex, a layer strongly labeled by agonists in posterior area 23 is absent in anterior area 24, suggesting that this labeling is indeed present in layer IV.

The binding sites present in layer IV of primary sensory cortices might reveal nAChRs expressed directly by the cortical neurons or, instead, denote the existence of nAChRs present on the afferents from the thalamic sensory relays. The differential labeling intensity for nicotinic agonists (strong labeling for epibatidine and cytisine but only moderate labeling for nicotine) might depend on the presence of α3/6-containing receptors. Conflicting results have been reported on the presence of α3 mRNA in the monkey thalamus (Cimino et al., 1992; Han et al., 2000), and there are some reports on the presence of α3 in the rodent embryonic or adult cortex (Wada et al., 1989; Zoli et al., 1995). Overall, the available data are still scanty, and the issue of composition and origin of nicotinic binding in layer IV of the monkey neocortex will require further investigation.

Conflicting reports have been published about α7 mRNA in the lateral geniculate, some authors detecting it (Quik et al., 2000a) and others not (Han et al., 2000). The primary visual cortex is the only cortical region where bungarotoxin labels layer IV. The hypothesis of receptors present on geniculate afferents is therefore plausible.

The strong and widespread labeling we observed for α-bungarotoxin in cortical layer I revealed the presence of an important population of α7 receptors in this area. They can be presynaptic receptors, located on axons coming from pyramidal neurons of layer II and III of the surrounding, or more remote, areas, and/or postsynaptic receptors, located on the apical dendritic tufts of pyramidal cells. In either case, α7-containing nAChRs could play a major role in the modulation of the processing of various signals in this layer, viewed as an integrating system. Such an integration of signals could help in building a global workspace (Dehaene et al., 1998) involved in the resolution of effortful cognitive tasks.

Here we have described an extensive autoradiographic mapping of [^{3}H]nicotine, [^{3}H]cytisine, [^{3}H]epibatidine, and [^{125}I]α-bungarotoxin binding sites in the brain of the rhesus monkey. Overall, the distribution of the binding sites for nicotine, cytisine, and epibatidine is similar in monkey and rodent brain. However, in the monkey, nicotinic agonist labeling correlates with the expression of α2, rather than α4 subunit as in the rodent. Moreover, the distribution of α-bungarotoxin binding sites, in agreement with what was previously shown for the α7 subunit mRNA (Han et al., 2000), is larger than that in the rodent brain, suggesting that this nAChR subtype may have a more important role in primates. Altogether, these findings show that rodents are only imperfect models for understanding the function of nicotinic receptors in primate brains and a fortiori in the human brain.

ACKNOWLEDGMENTS

We are grateful to Jean-Luc Charieau for help in animal handling and Clément Léna for useful discussions.

LITERATURE CITED

Adler LE, Olincy A, Waldo M, Harris JG, Griffith J, Stevens K, Flach K, Nagamoto H, Bickford P, Leonard S, Freedman R. 1998. Schizophrenia, sensory gating, and nicotinic receptors. Schizophr Bull 24:189–202.

Alonso JR, Amaral DG. 1995. Cholinergic innervation of the primate hippocampal formation. I. Distribution of choline acetyltransferase immunoreactivity in the *Macaca fascicularis* and *Macaca mulatta* monkeys. J Comp Neurol 355:135–170.

Alonso JR, Hoi Sang U, Amaral DG. 1996. Cholinergic innervation of the primate hippocampal formation: II. Effects of fimbria/fornix transection. J Comp Neurol 375:527–551.

Anand R, Peng X, Ballesta JJ, Lindstrom J. 1993. Pharmacological characterization of α-bungarotoxin-sensitive acetylcholine receptors immunoisolated from chick retina: contrasting properties of α7 and α8 subunit-containing subtypes. Mol Pharmacol 44:1046–1050.

Boulter J, Connolly J, Deneris E, Goldman D, Heinemann S, Patrick J. 1987. Functionnal expression of two neuronal nicotinic acetylcholine receptors from cDNA clones identifies a gene family. Proc Natl Acad Sci USA 84:7763–7767.

Breese CR, Adams C, Logel J, Drebing C, Rollins Y, Barnhart M, Sullivan B, Demasters BK, Freedman R, Leonard S. 1997. Comparison of the regional expression of nicotinic acetylcholine receptor alpha7 mRNA and [^{125}I]alpha-bungarotoxin binding in human postmortem brain. J Comp Neurol 387:385–398.

Broides RS, Robertson RT, Leslie FM. 1996. Regulation of α7 nicotinic acetylcholine receptors in the developing rat somatosensory cortex by thalamocortical afferents. J Neurosci 16:2956–2971.

Champtiaux N, Han Z-Y, Bessis A, Rossi FM, Zoli M, Marubio L, McIntosh M, Changeux J-P. 2002. Distribution and pharmacology of α6-containing nicotinic acetylcholine receptors analysed with mutant mice. J Neurosci 22:1208–1217.

Chen DN, Patrick J. 1997. The α-bungarotoxin-binding nicotinic acetylcholine receptor from rat brain contains only the α7 subunit. J Biol Chem 272:24024–24029.

Cimino M, Marini P, Fornasari D, Cattabeni F, Clementi F. 1992. Distribution of nicotinic receptors in cynomolgus monkey brain and ganglia—localization of alpha3 subunit messenger RNA, alpha-bungarotoxin and nicotine binding sites. Neuroscience 51:77–86.

Clarke PBS, Pert CB, Pert A. 1984. Autoradiographic distribution of nicotinic receptors in rat brain. Brain Res 323:390–395.

Clarke PBS, Schwartz RD, Paul SM, Pert CB, Pert A. 1985. Nicotinic binding in rat brain: Autoradiographic comparison of [^{3}H]acetylcholine, [^{3}H]nicotine, and [^{125}I]α-bungarotoxin. J Neurosci 5:1307–1315.

Corringer PJ, Le Novère N, Changeux J-P. 2000. Nicotinic receptors at the amino acid level. Annu Rev Pharmacol Toxicol 40:431–458.

Court J, Spurden D, Lloyd S, Mckeith I, Ballard C, Cairns N, Kerwin R, Perry R, Perry E. 1999. Neuronal nicotinic receptors in dementia with Lewy bodies and schizophrenia: a-bungarotoxin and nicotine binding in the thalamus. J Neurochem 73:1590–1597.

Court JA, Martin-Ruiz C, Graham A, Perry E. 2000a. Nicotinic receptors in human brain: topography and pathology. J Chem Neuroanat 20:281–298.

Court JA, Piggott MA, Lloyd S, Cookson N, Ballard CG, McKeith IG, Mckeith IG, Perry RH, Perry EK. 2000b. Nicotine binding in human striatum: elevation on schizophrenia and reductions in dementia with Lewy bodies, Parkinson's disease and Alzheimer's disease and in relation to neuroleptic medication. Neuroscience 98:79–87.

Court J, Martin-Ruiz C, Piggott M, Spurden D, Griffiths M, Perry E. 2001. Nicotinic receptor abnormalities in Alzheimer's disease. Biol Psychiatry 49:175–184.

Couturier S, Bertrand D, Matter J-M, Hernandez M-C, Bertrand S, Millar N, Valera S, Barkas T, Ballivet M. 1990. A neuronal nicotinic acetylcholine receptor subunit (α7) is developmentally regulated and forms homooligomeric channel blocked by α-Bgt. Neuron 5:847–856.

Crumeyrolle-Arias M, Jafarian-Tehrani M, Cardona A, Edelman L, Roux P, Laniece P, Charon Y, Haour F. 1996. Radioimagers as an alternative to film autoradiography for in situ quantitative analysis of ^{125}I-ligand receptor binding and pharmacological studies. Histochem J 28:801–809.

De Fusco M, Becchetti A, Patrignani A, Annesi G, Gambardella A, Quattrone A, Ballabio A, Wanke E, Casari G. 2000. The nicotinic receptor β2 subunit is mutant in nocturnal frontal lobe epilepsy. Nat Genet 26: 275–276.

Dehaene S, Kerszberg M, Changeux J-P. 1998. A neuronal model of a global workspace in effortful cognitive task. Proc Natl Acad Sci USA 95:14529–14534.

Di Chiara G. 2000. Role of dopamine in the behavioural actions of nicotine related to addiction. Eur J Pharmacol 393:295–314.

Freedman R, Hall M, Adeler LE, Leonard S. 1995. Evidence in postmortem brain tissue doe decreased number of hippocampal nicotinic receptors in Schizophrenia. Biol Psychiatry 38:22–33.

Freedman R, Coon H, Myles-Worsley M, Orr-Urtreger A, Olincy A, Davis A, Polymeropoulos M, Holik J, Hopkins J, Hoff M, Rosenthal J, Waldo MC, Reimherr F, Wender P, Yaw J, Young DA, Breese CR, Adams C, Patterson D, Adler LE, Kruglyak L, Leonard S, Byerley W. 1997. Linkage of a neurophysiological deficit in schizophrenia to a chromosome 15 locus. Proc Natl Acad Sci USA 94:587–592.

Fuchs JL. 1989. [^{125}I]α-bungarotoxin binding marks primary sensory areas of developing rat neocortex. Brain Res 501:223–234.

Gopalakrishnan M, Monteggia LM, Anderson DJ, Molinari EJ, Piattoni-Kaplan M, Donnelly-Roberts D, Arneric SP, Sullivan JP. 1996. Stable expression, pharmacologic properties and regulation of the human neuronal nicotinic acetylcholine α4β2 receptor. J Pharmacol Exp Ther 276:289–297.

Gotti C, Fornasari D, Clementi F. 1997. Human neuronal nicotinic receptors. Neurobiology 53:199–237.

Han Z-Y, Le Novère N, Zoli M, Hill JA Jr, Champtiaux N, Changeux J-P. 2000. Localization of nAChR subunit mRNA in the brain of *Macaca mulatta*. Eur J Neurosci 12:3664–3674.

Happe HK, Peters JL, Bergman DA, Murrin LC. 1994. Localization of nicotinic cholinergic receptors in rat brain: autoradiographic stidies with [^{3}H]cytisine. Neuroscience 62:929–944.

Härfstrand A, Adem A, Fuxe K, Agnati L, Andersson K, Nordberg A. 1988. Distribution of nicotinic cholinergic receptors in the rat tel- and diencephalon: a quantitative receptor autoradiographical study using [^{3}H]acetylcholine, [α-^{125}I]bungarotoxin and [^{3}H]nicotine. Acta Physiol Scand 132:1–14.

Kageyama GH, Gallivan ME, Gallardo KA, Robertson RT. 1990. Relationships between patterns of acetylcholinesterase activity and geniculocortical terminal fields in developing and mature rat visual cortex. Brain Res Dev Brain Res 53:139–144.

Karlin A. 2002. Emerging structure of the nicotinic acetylcholine receptors. Nat Rev Neurosci 3:102–114.

Le Novère N, Corringer P-J, Changeux J-P. 2002. The diversity of subunit composition in nAChRs: evolutionary origins, physiological and pharmacological consequences. J Neurobiol 53:447–456.

Léna C, Changeux J-P. 1997. Pathological mutations of nicotinic receptors and nicotine-based therapies for brain desorders. Curr Opin Neurobiol 7:674–682.

Levin E, Simon B. 1998. Nicotinic acetylcholine involvement in cognitive function in animals. Psychopharmacology 138:217–230.

Marubio LM, Arroyo-Jimenez MdM, Cordero-Erausquin M, Léna C, Le Novère N, de Kerchove d'Exaerde A, Huchet M, Damaj MI, Changeux J-P. 1999. Reduced antinociception in mice lacking neuronal nicotinic receptor subunits. Nature 398:805–810.

Morel A, Garraghty PE, Kaas JH. 1993. Tonotopic organization, architectonic fields, and connections of auditory cortex in macaque monkeys. J Comp Neurol 335:437–459.

Morris R, Petrides M, Pandya DN. 1999. Architecture and connections of retrosplenial area 30 in the rhesus monkey (*Macaca mulatta*). Eur J Neurosci 11:2506–2518.

Orr-Urtreger A, Goldner FM, Saeki M, Lorenzo I, Goldberg L, De Biasi M, Dani JA, Patrick JW, Beaudet AL. 1997. Mice deficient in the alpha7 neuronal nicotinic acetylcholine receptor lack alpha-bungarotoxin binding sites and hippocampal fast nicotinic currents. J Neurosci 17: 9165–9171.

Parker MJ, Beck A, Luetje CW. 1998. Neuronal nicotinic receptor β2 and β4 subunits confer large differences in agonist binding affinity. Mol Pharmacol 54:1132–1139.

Pauly JR, Stitzel JA, Marks MJ, Collins AC. 1989. An autoradiographic analysis of cholinergic receptors in mouse brain. Brain Res Bull 22: 453–459.

Paxinos G, Huang XF, Toga AW. 2000. The rhesus monkey brain. New York: Academic Press.

Perry D, Kellar K. 1995. [^{3}H]epibatidine labels nicotinic receptors in rat brain: an autoradiographic study. J Pharmacol Exp Ther 275:1030–1034.

Perry EK, Court JA, Johnson M, Piggott MA, Perry RH. 1992. Autoradiographic distribution of [^{3}H]nicotine binding in human cortex: relative abundance in subicular complex. J Chem Neuroanat 5:399–405.

Perry EK, Morris CM, Court JA, Cheng A, Fairbairn AF, McKeith IG, Irving D, Brown A, Perry RH. 1995. Alteration in nicotine binding sites in Parkinson's disease: possible index of early neuropathology. Neuroscience 64:385–395.

Picciotto MR, Zoli M, Léna C, Bessis A, Lallemand Y, Le Novère N, Vincent P, Merlo-Pich E, Brulet P, Changeux J-P. 1995. Abnormal avoidance learning in mice lacking functional high-affinity nicotine receptor in the brain. Nature 374:65–67.

Picciotto MR, Zoli M, Rimondini R, Léna C, Marubio LM, Merlo-Pich E, Fuxe K, Changeux J-P. 1998. Acetylcholine receptors containing the β2 subunit are involved in the reinforcing properties of nicotine. Nature 391:173–177.

Quik M, Polonskaya Y, Gillespie A, Jakowec M, Lloyd GK, Langston JW. 2000a. Localization of nicotinic receptor subunit mRNAs in monkey brain by in situ hybridization. J Comp Neurol 425:58–69.

Quik M, Polonskaya Y, Gillespie A, Lloyd GK, Langston JW. 2000b. Differential alteration in nicotinic receptor α6 and β3 subunit messenger RNAs in monkey substantia nigra after nigrostriatal degeneration. Neuroscience 100:63–72.

Rogers S, Gahring L, Collins A, Marks M. 1998. Age-related changes in neuronal nicotinic acetylcholine receptor subunit alpha4 expression are modified by long-term nicotine administration. J Neurosci 18:4825–4832.

Role LW, Berg DK. 1996. Nicotinic receptors in the development and modulation of CNS synapses. Neuron 16:1077–1085.

Ross SA, Wong JY, Clifford JJ, Kinsella A, Massalas JS, Horne MK, Scheffer IE, Kola I, Waddington JL, Berkovic SF, Drago J. 2000. Phenotypic characterisation of an α4 neuronal nicotinic acetylcholine receptor subunit knock-out mouse. J Neurosci 20:6431–6441.

Rubboli F, Court J, Sala C, Morris C, Chini B, Perry E, Clementi F. 1994. Distribution of nicotinic receptors in the human hippocampus and thalamus. Eur J Neurosci 6:1596–1604.

Schilstrom B, Fagerquist, MV, Zhang X, Hertel P, Panagis G, Nomikos G, Svensson T. 2000. Putative role of presynaptic alpha7* nicotinic receptors in nicotine stimulated increases of extracellular levels of glutamate and aspartate in the ventral tegmental area. Synapse 38:375–383.

Schoepfer R, Conroy WG, Whiting P, Gore M, Lindstrom J. 1990. Brain alpha-bungarotoxin binding protein cDNAs and mAbs reveal subtypes of this branch of the ligand-gated ion channel gene superfamily. Neuron 5:35–48.

Séguéla P, Wadiche J, Dineley-Miller K, Dani J, Patrick JW. 1993. Molecular cloning, functional properties, and distribution ofrat brain alpha7: a nicotinic cation channel highly permeable to calcium. J Neurosci 13:596–604.

Sihver W, Gillberrg PG, Nordberg A. 1998. Laminar distribution of nicotinic receptor subtypes in human cerebral cortex as determined by [^{3}H]nicotine, [^{3}H]cytisine and [^{3}H]epibatidine in vitro autoradiography. Neuroscience 85:1121–1133.

Sihver W, Gillberg P-G, Svensson A-L, Nordberg A. 1999. Autoradiographic comparison of [^{3}H]nicotine, [^{3}H]cytisine and [^{3}H]epibatidine binding in relation to vesicular acetylcholine transport sites in the temporal cortex in Alzheimer's disease. Neuroscience 94:685–696.

Spurden DP, Court JA, Lloyd S, Oakley A, Perry R, Pearson C, Pullen RGL, Perry EK. 1997. Nicotinic receptor distrinution in the human thalamus: autoradiographical localization of [^{3}H]nicotine and [^{125}I]α-bungarotoxin binding. J Chem Neuroanat 13:105–113.

Stauderman KA, Mahaffy LS, Akong M, Veliçelebi G, Chavez-noriega LE, Crona JH, Johnson EC, Elliott KJ, Gillespie A, Reid RT, Adams P, Harpold MM, Corey-Naeve J. 1998. Characterization of human recombinant neuronal nicotinic acetylcholine receptor subunit combinations α2β4, α3β4 and α4β4 stably expressed in HEK293 Cells. J Pharmacol Exp Ther 284:777–789.

Steinlein O, Mulley J, Propping P, Wallace R, Phillips H, Sutherland G, Scheffer I, Berkovic S. 1995. A missense mutation in the neuronal nicotinic acetylcholine receptor alpha 4 subunit is associated with autosomal dominant nocturnal frontal lobe epilepsy. Nat Genet 11: 201–203.

Steinlein OK, Magnusson A, Stoodt J, Bertrand S, Weiland S, Berkovic S, Nakken K, Propping P, Bertrand D. 1997. An insertion mutation of the CHRNA4 gene in a family with autosomal dominant nocturnal frontal lobe epilepsy. Hum Mol Genet 6:943–947.

Szabo J, Cowan WM. 1984. A stereotaxic atlas of the brain of the cynomologous monkey (*Macaca fascicularis*). J Comp Neurol 222:265–300.

Wada E, Wada K, Boulter J, Deneris E, Heinemann S, Patrick J, Swaanson LW. 1989. Distribution of alpha2, alpha3, alpha4, and beta2 neuronal nicotinic receptor subunit mRNAs in the central nervous system: a hybridization histochemical study in the rat. J Comp Neurol 184:314–335.

Wang F, Gerzanich V, Wells GB, Anand R, Peng X. 1996. Assembly of human neuronal nicotinic receptor alpha5 subunits with alpha3, beta2 and beta4. J Biol Chem 271:17656–17665.

Whiteaker P, Davies ARL, Marks MJ, Blagbrough IS, Potter BVL, Wolstenholme AJ, Collins AC, Wonnacott S. 1999. An autoragraphic study of the distribution of binding sites for the novel a7-selective nicotinic radioligand [^{3}H]methyllycaconitine in the mouse brain. Eur J Neurosci 11:2689–2696.

Whiting P, Schoepfer R, Lindstrom J, Priestley T. 1991. Structural and pharmacological characterization of the major brain nicotinic acetylcholine receptor subtype stably expressed in mouse fibroblast. Mol Pharmacol 40:463–472.

Zoli M, Le Novère N, Hill JA, Changeux J-P. 1995. Developmental regulation of nicotinic ACh receptor subunit mRNAs in the rat central and peripheral nervous systems. J Neurosci 15:1912–1939.

Zoli M, Léna C, Picciotto MR, Changeux J-P. 1998. Identification of four classes of brain nicotinic receptors using β2 mutant mice. J Neurosci 18:4461–4472.

Zoli M, Picciotto MR, Ferrari R, Cocchi D, Changeux J-P. 1999. Increased neurodegeneration during ageing in mice lacking high-affinity nicotine receptors. EMBO J 18:1235–1244.